20, 1172), is split into a doublet peak (86.5 and 78.0 ppm) with a peak separation of 8.5 ppm (unpublished). At present, however, we assume the C-4 signal of the type II salt to be a singlet, unless new evidence is obtained.

(38) The lattice angles of the two peaks, 11.5° and 16.4°, are both a little larger than those observed at 100% relative humidity, 11.2° and 16.0°, respectively. These are equatorial reflections [the former is of (020) and (120) and the latter of (220) and (030) reflections, respectively] and change with relative humidity;[3] e.g., under vacuum, the former became 12.8. The present X-ray measurements were carried out at room humidity, ca. 40% relative humidity.

Complexation Chemistry of Sodium Borate with Poly(vinyl alcohol) and Small Diols. A ^{11}B NMR Study

Steve W. Sinton†

Exxon Production Research Company, Houston, Texas 77252-2189.
Received October 31, 1986

ABSTRACT: ^{11}B nuclear magnetic resonance spectroscopy was used to study the complexation chemistry of sodium borate (SB) with several organic polyols, including poly(vinyl alcohol) (PVA), in water. The cross-link structure in the PVA/SB system is deduced by comparison of diol/SB and PVA/SB spectra. Results are interpreted in terms of equilibrium constants, activation energies, and enthalpies for the various reactions involved. There are two ^{11}B signal components from PVA/SB solutions which can be assigned to cross-linking complexes. These two components are shown to have different spin relaxation rates. This behavior is discussed in terms of the mechanism for ^{11}B NMR relaxation and the polymer chain motions. Relationships between NMR parameters and viscosity in the PVA/SB system are discussed. It is concluded that certain theoretical descriptions of viscosity in associating polymer systems might be tested by combining mechanical and NMR measurements on the PVA/SB system.

Introduction

Sodium borate (SB) as common borax ($Na_2B_4O_7 \cdot 10H_2O$) at low concentrations in water dissociates completely into boric, $B(OH)_3$, and monoborate, $B(OH)_4^-$, molecules.[1] The acid/base equilibrium between these two species,

$$B(OH)_3 + H_2O \underset{k_{-1}}{\overset{k_1}{\rightleftharpoons}} B(OH)_4^- + H^+ \qquad (1)$$

has an equilibrium constant $pK_a = 9$.[2] In what follows, $B(OH)_3$ and $B(OH)_4^-$ are occasionally abbreviated as B and B^-, respectively. It has long been known that monoborate anions complex certain organic polyols according to eq 2 and 3.[3-10]

$$A + B^- \rightleftarrows AB^- + 2H_2O \qquad (2)$$

$$2A + B^- \rightleftarrows A_2B^- + 4H_2O \qquad (3)$$

In these equilibria the symbols A, AB^-, and A_2B^-, represent free polyol and polyol/monoborate complexes with 1:1 and 2:1 stoichiometry. For 1,3-type hydroxyl substitution on a linear hydrocarbon chain (e.g., poly(vinyl alcohol)) (PVA), complexation involves attachment of boron to adjacent oxygens, forming structures I and II for AB^- and A_2B^-, respectively.

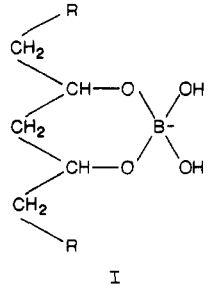

I

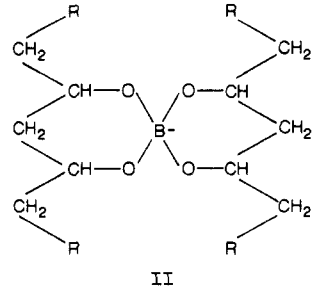

II

†Present address: Lockheed Missiles and Space Co., D/9350 B/204, 3251 Hanover St., Palo Alto, CA 94304.

Cross-linking caused by formation of 2:1 complexes has been cited as the chemical basis of enhanced viscosification in PVA/SB solutions.[11-14] Savins[11] attributed unusual rheological behavior of some PVA/SB compositions to a shear dependence in the formation of 2:1 complexes. Maerker and Sinton[14] extended this work to show that certain PVA/SB compositions result in shear-thickening and shear-thinning fluids. Shultz and Myers[12] calculated enthalpies for complexation from temperature-dependent dynamic mechanical data on borate-cross-linked PVA gels. Nickerson[13] argued from their results and his pH data that hydrogen bonding between polymer and monoborate anions and not 2:1 complexation must be responsible for viscosification and gelation effects in this system. More recently, the existence of PVA–borate complexes has been demonstrated with ^{11}B NMR.[14] NMR is a particularly useful technique because ^{11}B chemical shifts are sensitive to the oxygen symmetry (trigonal or tetrahedral) about boron[15,16] and to the size of polynuclear rings in 1:1 and 2:1 complexes.[8]

The work reported here was undertaken with two major goals in mind. First, it is desirable to fully characterize the complexation chemistry expressed by eq 1 and 2 and for this purpose a more thorough NMR study was performed. The second goal is to combine this chemical information with rheological data on PVA/SB solutions in order to develop a descriptive model of viscosity for such a solution. This paper is concerned primarily with the complexation chemistry while some results are discussed in terms of the relationship between chemistry and viscosity. The rheology of the PVA/SB system is covered in greater detail elsewhere.[11,12,14]

Several aspects of the complexation chemistry were studied in detail by using low-molecular-weight diols in addition to PVA. ^{11}B chemical shift assignments were easily made with these simple diols and were then useful for signal assignment in the PVA/SB case. A detailed picture of the chemistry involved in diol/SB systems was

0024-9297/87/2220-2430$01.50/0

obtained and used for comparison in the study of the PVA/SB system. In addition, certain effects of chain configuration on complexation were checked by choosing appropriate diols. For example, borate complexation is usually specific for molecules with hydroxyls in a cis-type arrangement. Since PVA is a flexible chain, all conformations of adjacent C–O vectors are conceivably possible. Steric and Coulombic interactions make the various conformations energetically inequivalent. These interactions depend on whether the monomer pair (or "diad") has a meso or racemic stereochemical configuration.[17] Thus, one might expect complexation with one diad variety to be more difficult than with the other. 2,4-Pentanediol was chosen as a simple "dimer" analogue to PVA diads. Experiments were conducted with an isomer mixture of 2,4-pentanediol and purified 2*R*,4*R* isomer to determine what role, if any, stereochemistry plays in the PVA/SB system. Other diols in solution with SB were also studied to see what effect the chain length between neighboring hydroxyls has on complexation. Results with these simple diols are compared to PVA/SB spectra to confirm structure II for the cross-links.

The results and discussions which follow are arranged in three sections. In the first, aqueous borate speciation is reviewed with examples of ^{11}B spectra of SB solutions without any polyol. Some new variable-temperature results are also reported in this section. The discussion of NMR parameters in this section is necessary to develop interpretations of polyol/SB spectra in the second and third sections. The second section covers borate complexation by simple (low-molecular-weight) diols. The third section presents the PVA/SB results. Chemical shifts, equilibrium constants, and exchange effects for this case are compared to the diol/SB results. The NMR data are examined in light of viscosity trends in the PVA/SB system.

Experimental Section

Sodium borate decahydrate, 2,4-pentanediol (2,4-PD), 1,5-pentanediol (1,5-PD), and 2,3-butanediol (2,3-BD) were purchased from Aldrich Chemicals and used without further purification. Four different polymers were used as obtained from either Aldrich or Scientific Polymer Products: PVA88 (88% hydrolyzed, average MW 125 000); PVA96 (96% hydrolyzed, average MW 95 000); PVA100 (100% hydrolyzed, average MW 14 000); PVA98 (98% hydrolyzed, average MW 16 000). NaOH and HCl solutions were prepared with chemicals purchased from Fisher Scientific. Deionized or deionized–distilled water was used in the preparation of all solutions.

Stock polymer solutions were prepared by dissolving the appropriate amount of polymer in water while stirring. Complete dissolution usually occurred within a few days. PVA88 and PVA96 formed clear solutions at room temperature while PVA98 and PVA100 required heating (80 °C). Each stock solution was filtered through nylon mesh (70-μm openings) prior to use. Proton-decoupled ^{13}C NMR of the PVA stock solutions was used to check polymer tacticity. Although precise tacticity determinations were not attempted, these spectra qualitatively matched literature results for atactic PVA.[18-21] All polymer concentrations are given in weight percent.

Measurements of pH were made with a Corning Model 135 meter using a gel-filled polymer–body combination electrode (Fisher). Accuracy was estimated to be about ±0.02 pH units. Several minutes were typically allowed for stabilization before recording pH of PVA/SB samples as the values tended to drift noticeably.

NMR spectra were collected with a Bruker CXP 300 Fourier transform spectrometer operating at 96.3 MHz for ^{11}B (7.05-T superconducting magnet). All samples were contained in quartz 10-mm tubes. A low-Q probe was employed so as to minimize interference between rapidly decaying NMR signals and transient electrical responses to radiofrequency pulses. Although this probe has a glass insert, a ^{11}B background signal could not be detected. Typical acquisition parameters were 90° pulse duration, 32 μs; spectral width, 5 kHz; data size, 1024 words; relaxation delay, 100 ms; and number of shots, 1000–10 000. Field stability was such that no field-frequency lock was required. It was not necessary to spin samples to remove the effects of field inhomogeneity as line shapes are dominated by other effects. Except for variable-temperature experiments, sample temperature was at the ambient room value (approximately 24 °C). In variable-temperature runs, sample temperature regulation within ±1 °C was achieved with a Bruker BVT-1000s unit. Peak areas for spectra with resolved line shapes were calculated with the standard NMR integration software. For unresolved lines, peak areas were obtained with an interactive computer program (supplied by Bruker) which allows the operator to fit experimental line shapes with a series of Lorentzian functions. Root-mean-square deviations between fitted and experimental line shapes are typically below 15%. Spectra for relaxation experiments were acquired with the standard inversion–recovery (π–τ–$\pi/2$–acquire) sequence. ^{11}B chemical shifts were measured relative to external $BF_3O(C_2H_5)_2$ with positive values for signals at higher frequency than this reference. Accuracy of all chemical-shift determinations is estimated to be ±0.2 ppm. Susceptibility corrections for externally referenced ^{11}B shifts are usually small[15,16] and so were not applied.

Viscosity measurements were made with a Rheometrics Fluids Rheometer using a cone-and-plate geometry. Detailed descriptions of the setup and typical experimental parameters are given elsewhere.[14]

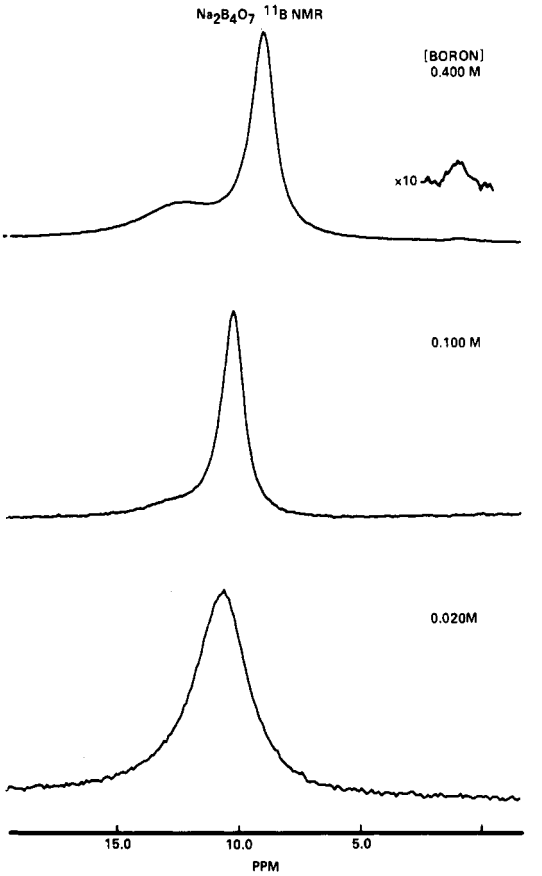

Figure 1. ^{11}B NMR spectra of SB at three concentrations. Chemical shift scale is referenced to external $BF_3O(C_2H_5)_2$. Total boron concentration is indicated above each spectrum.

Results and Discussion

Aqueous Borate Speciation. Figure 1 shows ^{11}B spectra for three different concentrations of SB in water. At the highest concentration, several species exist with sufficiently long lifetimes to give separate signals (top spectrum of Figure 1). These species have been identified by several techniques and ^{11}B chemical shifts assigned over the years by different groups.[22-26] The most prominent

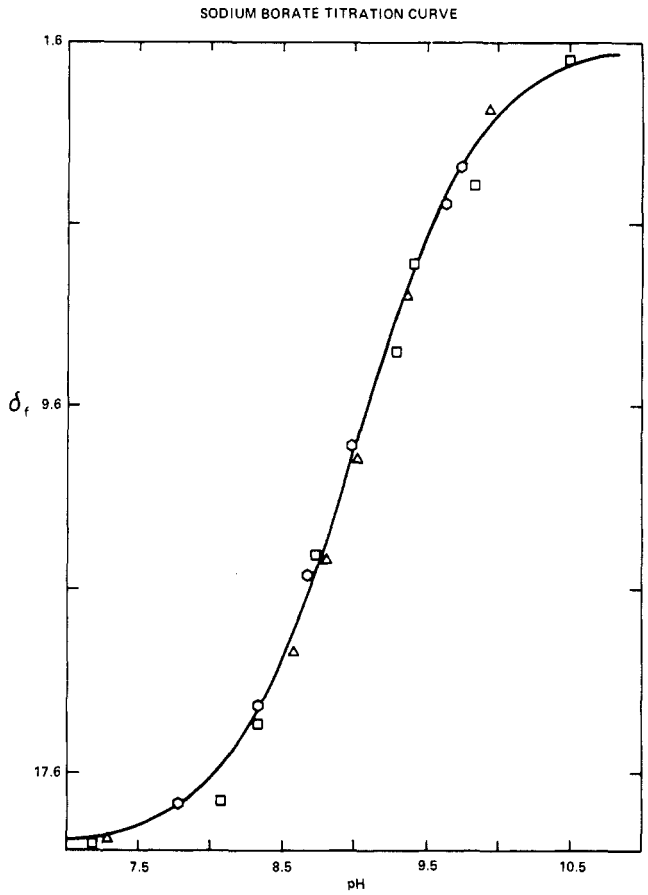

Figure 2. Variation of boric/monoborate ^{11}B chemical shift with pH for SB solutions at various total boron concentrations: 0.01 M (squares); 0.02 M (triangles); 0.05 M (hexagons).

peak in Figure 1 at high concentration arises from boron in the boric $B(OH)_3$ and monoborate $B(OH)_4^-$ species which are exchanging rapidly according to eq 1. The other signals at high concentration have been attributed to boron in polyborate species formed by polymerization of the monomeric molecules.[22-26]

As total boron concentration decreases, polyborate concentrations decrease. At 0.05 M boron and lower concentrations, only the boric/monoborate ^{11}B NMR signal is detectable (Figure 1, bottom). This peak is substantially broader than the corresponding peak at higher concentrations indicating slower exchange between $B(OH)_3$ and $B(OH)_4^-$ at the lower concentration. The exchange is still sufficiently rapid so that only the average shift, δ_f, is observed according to eq 4. In this expression, X_B and X_{B^-}

$$\delta_f = X_B\delta_B + X_{B^-}\delta_{B^-} \quad (4)$$

are the mole fractions of $B(OH)_3$ and $B(OH)_4^-$, respectively, and δ_B, δ_{B^-} are chemical shifts of the pure species.

The chemical shift of the boric/borate peak should be related to pH and the acid constant for $B(OH)_3$ by eq 5:[24]

$$pH = \log (X) + pK_a \quad (5)$$

where

$$X = \frac{\delta_f - \delta_B}{\delta_{B^-} - \delta_f} \quad (6)$$

Equation 5 is verified by the data plotted in Figure 2. This figure shows that the pH/chemical-shift correlation is independent of concentration (as predicted) for solutions below a concentration where polyborate NMR signals are observed, confirming that only the monomeric species exist at these concentrations. The solid curve in Figure 2 is a

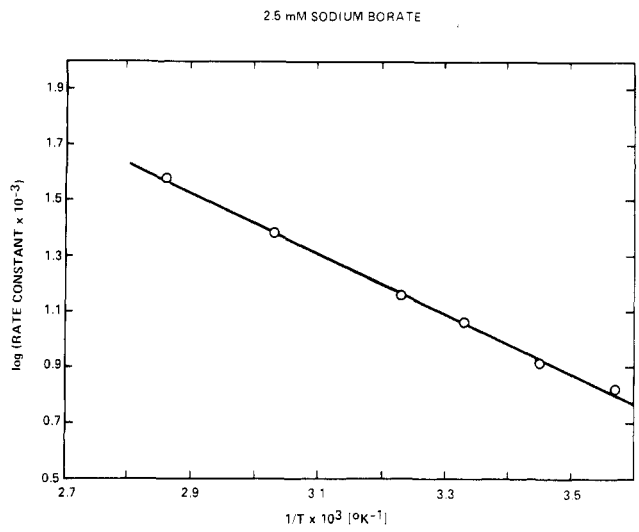

Figure 3. Arrhenius plot of logarithm of the rate of constant vs. $1/T$ from the boric/monoborate exchange peak of 2.5 mM SB (0.01 M total boron).

plot of eq 5 with $pK_a = 9.0$, $\delta_B = 19.3$ ppm, and $\delta_{B^-} = 1.6$ ppm.

The line width of the boric/monoborate peak is temperature dependent at low boron concentrations; this line narrows with increasing temperature. The peak position, however, does not vary appreciably from 280 to 350 K. The line-width variation was interpreted by considering a simple two-site model for exchange of boron between trigonal and tetrahedral forms according to the equilibrium expressed in eq 1. Forward and reverse rate constants for this exchange (k_1 and k_{-1}, respectively) can be calculated as outlined in the Appendix. Since the peak position is constant over the temperature range studied, it is a good approximation to take K_a as constant and the exchange barriers for forward and reverse directions of eq 1 as equal. The activation energy E_a was extracted from the temperature dependence of the exchange through the Arrhenius equation

$$k_1 = k_{-1}K_a = A \exp(-E_a/RT) \quad (7)$$

where R is the gas constant. Figure 3 is a plot of log k_1 against $1/T$. E_a calculated from the slope of the linear fit is 4.9 ± 0.2 kcal/mol.

Broadening of the boric/monoborate peak as boron concentration decreases indicates that the exchange rate is controlled by diffusion at low concentrations. There are two possible sources of the activation energy for interconversion between these species: the barrier to diffusion and the barrier to conversion between trigonal and tetrahedral coordination. The latter process involves attachment of OH^- and a hybridization change for boron and probably does not require a large amount of energy. From the data alone, one cannot separate contributions to the activation energy from these two sources. The close fit obtained by using the two-site model indicates that one can consider the exchange process to involve only a single activation energy within the temperature range studied.

These results can be summarized with the following generalizations concerning ^{11}B NMR of SB solutions: (1) the spectra reflect speciation of boron into boric, monoborate, and polyborate types; (2) the chemical shifts reflect the oxygen coordination of boron with tetrahedral boron appearing at lower shifts than trigonal boron; (3) at sufficiently low boron concentrations (equal to or less than 0.05 M), concentrations of polyborates are insignificant. (all results which follow are on solutions at or below this limit); (4) exchange effects are important to a full un-

Table I
^{11}B NMR Parameters[a] for Diol/SB Solutions

		free boron			1:1 complexes			2:1 complexes		
(n_D/n_B)[b]	pH	δ_f	W_f	A_f	δ_1	W_1	A_1	δ_2	W_2	A_2
				2,4-Pentanediol						
1.15	9.09	10.9	250	96	2.1	60	4			
2.70	9.11	11.3	250	92	2.3	60	8			
11.50	9.00	12.9	270	78	2.6	80	22			
25.00	8.52	15.1	380	66	3.4	190	34			
40.00	8.45	16.0	350	57	3.9	220	36	1.8[c]	250	7
50.00	8.40	16.7	350	57	4.3	250	37	1.8[c]	160	6
45.60*	8.93	17.5	290	36	5.9	350	58	1.5	100	6
				2,3-Butanediol						
1.10	8.75	12.2	280	84	4.9	20	14	8.3	50	2
2.75	8.59	14.5	290	69	5.0	20	24	8.4	50	7
5.50	8.33	16.5	250	58	4.9	20	25	8.3	50	17
10.00	7.90	18.1	160	52	5.1	30	22	8.3	50	26
25.50	7.40	19.0	110	49	5.7	60	13	8.3	50	38
10.00*	7.00	18.9	100	49	5.5	40	14	8.2	50	37

[a] δ_f, δ_1, and δ_2 are chemical shifts (in ppm) referenced externally to $BF_3O(C_2H_5)_2$ and assigned to free boron, 1:1 complexes, and 2:1 complexes, respectively. W_f, W_1, and W_2 are the corresponding line width (fwhm in Hz, estimated precision ±20 Hz). Peak areas (A_f, A_1, and A_2) are given as relative percentages of the total area. [b] Diol-to-boron mole ratio. For all solutions except those marked with an asterisk, total boron concentration was 0.02 M. For solutions marked with an asterisk, total boron concentration was 0.05 M. [c] This signal appears as an unresolved shoulder of the δ_1 peak.

derstanding of the NMR parameters.

Borate Complexation with Low-Molecular-Weight Diols. 2,4-PD/SB Solutions at Low Diol Concentration. Figure 4 shows ^{11}B spectra of SB solutions with various amounts of 2,4-pentanediol. Table I contains the NMR parameters and pH data from a number of 2,4-PD/SB samples. At low 2,4-PD concentrations, the spectra (Figure 4A,B) consist of two lines: a boric/monoborate exchange peak (henceforth referred to as the "free-boron" peak) and a second line between 2 and 3 ppm. The position of the latter peak is consistent with tetrahedral boron in a structure such as I or II. As shown below, this line position is actually affected by chemical exchange.

Increasing the 2,4-PD concentration caused the free-boron peak to move toward higher chemical shifts. This is consistent with the equilibria written above provided that at least one of the complexation constants is larger than K_a. Contrasting with this result is the pH trend in Table I. Low concentrations of 2,4-PD lead to a measured pH slightly above 9.00. Higher concentrations of 2,4-PD reveal that δ_f does not relate to pH through eq 5 with pK_a = 9. The relationship between pH and free-boron chemical shift is discussed in more detail in a later section.

2,4-PD/SB Solutions at High Diol Concentration. As the mole ratio of 2,4-PD to boron was raised above 11.5, the δ_1 peak broadened and developed a shoulder (see Table I). At certain combinations of pH and concentration, this shoulder became a separate peak at about 1–2 ppm (Figure 4C). The position and concentration dependence of this peak allow its assignment to 2:1 2,4-PD/monoborate complexes. A similar interpretation of propanediol/SB ^{11}B chemical shifts was given by Henderson and colleagues.[8]

Stereoselectivity. The pentanediol used in the experiments discussed above is a mixture of three stereoisomers: 2*S*,4*S*; 2*R*,4*R*; and 2*R*,4*S*. The 2*S*,4*S* and 2*R*,4*R* isomers have the same stereochemical configuration as racemic diads of PVA while the 2*R*,4*S* isomer configuration matches that of meso PVA diads. Purified 2(*R*),4(*R*)-pentanediol was used to check for stereoselectivity in the complexation reactions. The results are shown in Figure 5. Evidently, the 2*R*,4*R* isomer does not react with SB appreciably at this concentration level. The small peak at about 1 ppm in Figure 5C may be a result of isomeric impurity in the pentanediol (reportedly 99% 2*R*,4*R* isomer). Carbon-13 and proton NMR of these solutions confirmed the stereoselectivity result.

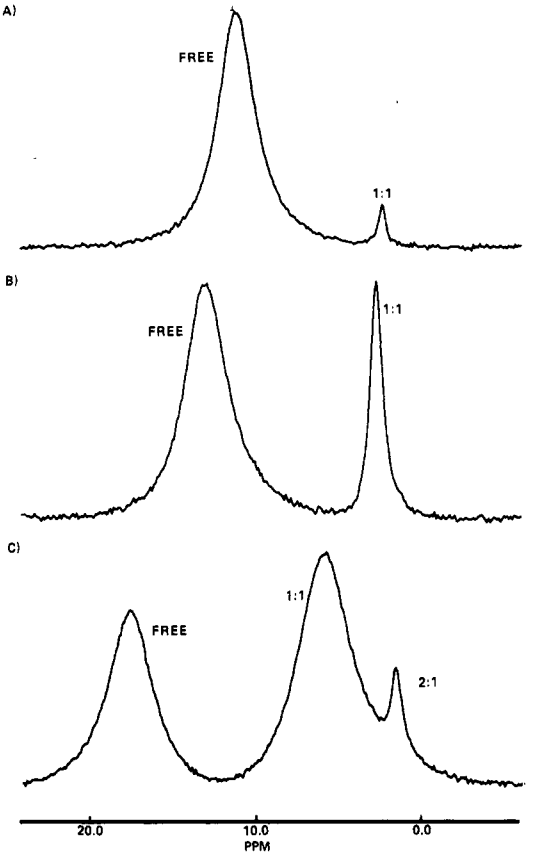

Figure 4. ^{11}B NMR spectra of 2,4-PD/SB solutions. Chemical shift assignments are explained in the text. (A) [2,4-PD] = 0.023 M, [boron] = 0.020 M; (B) [2,4-PD] = 0.230 M, [boron] = 0.020 M; (C) [2,4-PD] = 2.28 M, [boron] = 0.050 M.

Stereoselectivity is probably the result of steric interactions which make complexation with racemic configurations unfavorable. If the ring structure of the complex is placed in a chair conformation, both methyl groups are in an equatorial position for the meso isomer, whereas one methyl group would have to be in an axial position for the racemic isomers. More energy would be required for complexation of a racemic isomer in order to overcome steric forces on the axial methyl group in this conforma-

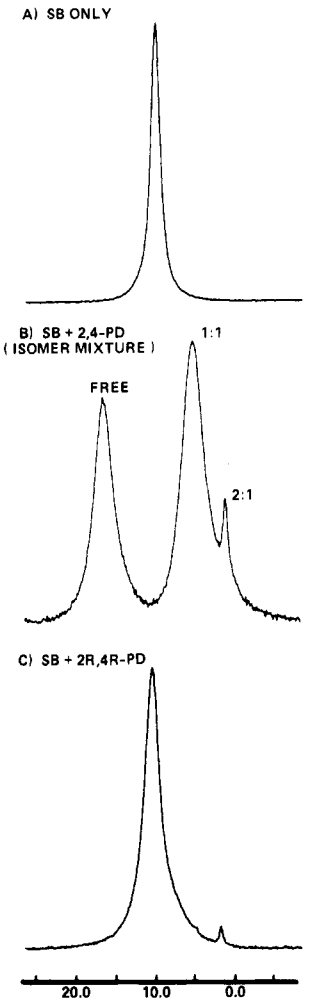

Figure 5. ^{11}B NMR spectra of SB solutions (0.05 M total boron) with (A) no diol, (B) 2.28 M 2,4-PD (isomer mixture), and (C) 1.19 M 2*R*,4*R*-PD. The complexation reactions are selective for the meso isomer.

tion. The situation should be similar for PVA where the methyls are replaced by the polymer chain. Thus, complexation should be selective for the meso diads of PVA.

Other Low-Molecular-Weight Diols. Figure 6 contains ^{11}B spectra from solutions of 1,5-pentanediol and 2,3-butanediol with SB. Narrow peaks from 1:1 and 2:1 complexes appear in the 2,3-BD/SB spectrum. Peak assignments in Figure 6B are consistent with the concentration dependence of peak areas in Table I. The appearance of a 2:1 complexed-boron peak at a higher chemical shift than the 1:1 peak has been reported by other groups[8-10] and attributed to the ring size of the complex by Henderson and colleagues.[8] In contrast to the result for 2,3-BD, no evidence of complexation was found for 1,5-PD; only the free-boron signal appears in Figure 6A. Complexation appears to be facile when five- or six-membered rings form but larger ring structures probably do not occur for flexible, linear polyols.

Equilibrium Constants. It is possible to calculate all species concentrations necessary to specify equilibrium constants for eq 2 and 3 from the NMR data in Table I. The method used is described in the Appendix and the results are listed in Table II. In the 2,4-PD/SB system, values of K_{C1}, the equilibrium constant for eq 2, are relatively constant at low diol concentration but vary for solutions that exhibited evidence of 2:1 complexation. This variation is either a result of poor resolution of the δ_1 and δ_2 peaks or an alteration in chemistry due to solvent effects (see below). Only the last solution ([2,4-PD]/[boron] =

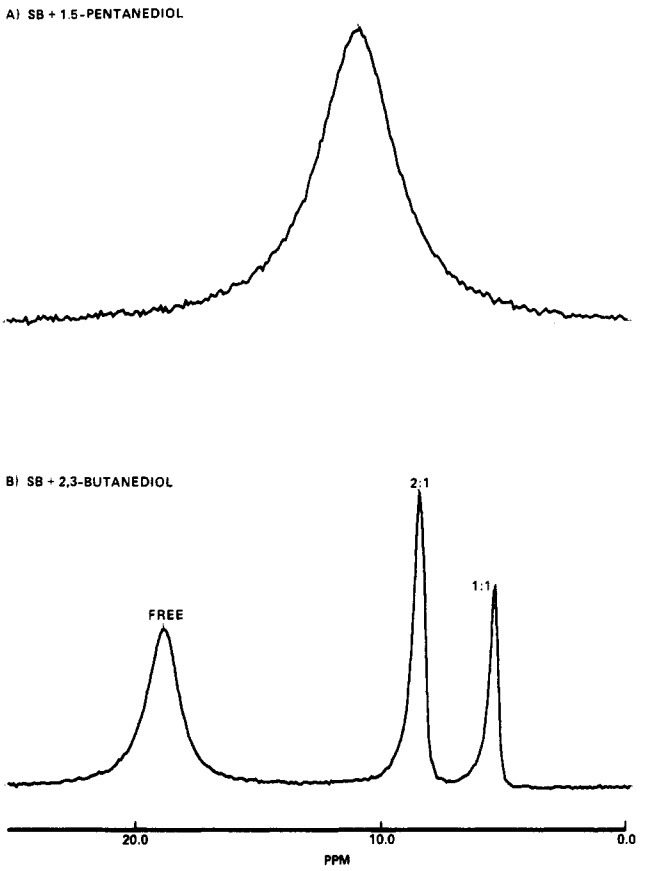

Figure 6. ^{11}B NMR spectra of SB solutions with (A) 0.24 M 1,5-pentanediol and (B) 0.28 M 2,3-butanediol. Total boron concentration was 0.02 M in both cases.

Table II
Equilibrium Constants[a] for Diol/Monoborate Complexation

$(n_D/n_B)^b$	K_{C1}/M^{-1}	K_{C2}/M^{-2}	$(n_D/n_B)^b$	K_{C1}/M^{-1}	K_{C2}/M^{-2}
		2,4-Pentanediol			
1.15	7.4		40.00	8.9	4.7
2.70	7.9		50.00	8.8	3.1
11.50	7.1		45.60*	14.2	1.3
25.00	9.0				
		2,3-Butanediol			
1.10	58	1010	10.00	75	1040
2.75	65	860	25.00	68	870
5.50	64	980	10.00*	64	770

[a] See Appendix for a definition of the equilibrium constants and details of the calculations. Temperature ~24 °C. [b] Diol-to-boron mole ratio. For all solutions except those marked with an asterisk, total boron concentration was 0.02 M. For solutions marked with an asterisk, total boron concentration was 0.05 M.

45.6) gave reasonably resolved 1:1 and 2:1 peaks, and the K_{C1} and K_{C2} values for this case are quite different than those determined for solutions with lower diol-to-boron ratios. In the 2,3-BD system, K_{C1} and K_{C2} agree reasonably well among all the different solutions tested. This diol is clearly more reactive than 2,4-PD toward monoborate complexation.

Values of K_{C1} and K_{C2} in Table II for 2,3-BD/SB do not agree with those of Roy et al.[3] determined by pH measurements (K_{C1} = 3.45, K_{C2} = 4.85). This discrepancy can be attributed to differences in experimental conditions and calculation methods. Roy et al. used a higher boron concentration (0.08 M) in which polyborate formation may not have been negligible. To obtain K_{C1}, they first measured pK_a without diol and then used this value with pH to calculate monoborate and complexed-boron concentrations. As I show in the next section, this method can

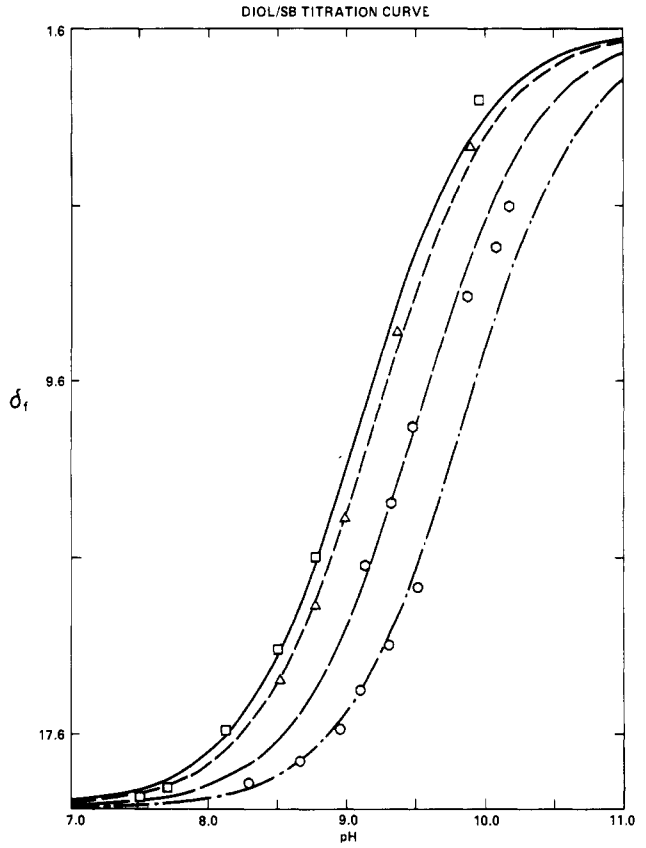

Figure 7. Variations of free-boron chemical shift with pH for several diol/SB solutions: 0.20 M 2,3-BD, 0.02 M boron (squares); 0.20 M 2,4-PD, 0.02 M boron (triangles); 2.28 M 2,4-PD, 0.05 M boron (circles); 2.00 M 1,5-PD, 0.05 M boron (hexagons). The curves were generated as explained in the text.

introduce errors because the relationship between measured pH and monoborate concentration changes with diol concentration. Roy et al. attempted to correct for these effects and obtain K_{C1} by extrapolating their results to zero diol concentration. They interpreted a composition variation in their uncorrected values of K_{C1} as evidence for 2:1 complexation and extracted K_{C2} from this variation. The NMR method gives K_{C1} and K_{C2} directly from δ_f and the peak peak areas and does not require a pH measurement. Finally, the equilibrium constants in Table II were calculated by assuming stereoselective complexation with meso 2,3-BD molecules. The diol concentration used was thus one-half of the total diol concentration (see Appendix). Roy et al. apparently based their calculations of K_{C1} and K_{C2} on the total diol concentration. Ignoring stereoselectivity effects decreases K_{C1} and K_{C2} in Table II by factors of about 2 and 4, respectively.

Titration Curves for Diol/SB Solutions. Plots of δ_f against pH for the three simple diols with SB are shown in Figure 7. Each set of data points comes from experiments at constant SB and diol concentrations with pH adjusted by addition of either HCl or NaOH. Overlap of free-boron and complexed-boron signals prevented determination of δ_f over the entire pH range for 2,3-BD and 2,4-PD. The calculated curves of Figure 7 were generated from eq 5 with pK_a = 9.10, 9.20, 9.50, and 9.84 for 0.20 M 2,3-BD/0.02 M boron, 0.20 M 2,4-PD/0.02 M boron, 2.00 M 1,5-PD/0.05 M boron, and 2.28 M 2,4-PD/0.05 M boron, respectively. Selected NMR spectra are shown for 2,4-PD and 2,3-BD in Figure 8.

Horizontal shifts of the titration curves might be the result of either systematic errors in pH measurements or a variation in pK_a with diol concentration. Both effects could conceivably happen since dielectric properties of the

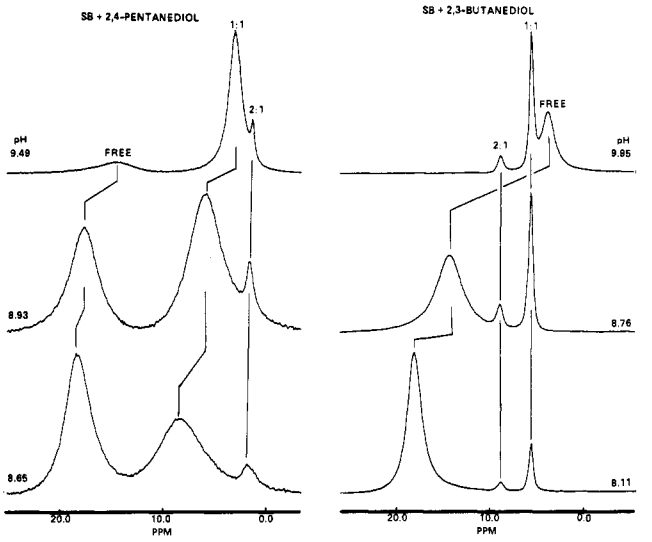

Figure 8. ^{11}B NMR spectra of diol/SB solutions at various pH values. Left: 2.28 M 2,4-PD, 0.05 M boron. Right: 0.20 M 2.3-PD, 0.02 M boron.

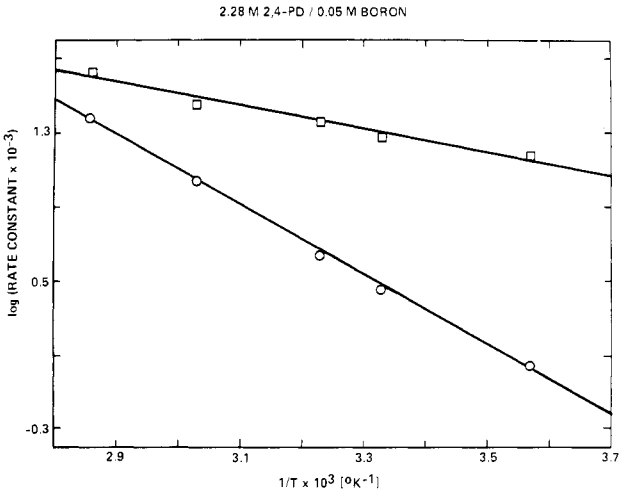

Figure 9. Arrhenius plots of free-boron (circles) and 1:1 complexed-boron (squares) rate constants calculated from the variable-temperature data on 2.28 M 2,4-PD, 0.05 M boron (Table III).

Table III
Temperature Dependence of NMR Parameters for 2,4-Pentanediol/SB[a]

	free boron			1:1 complexes			2:1 complexes		
T/K	δ_f	W_f	A_f	δ_1	W_1	A_1	δ_2	W_2	A_2
280	17.6	350	39	5.5	370	55	1.2	100	6
300	16.8	270	39	5.9	310	57	1.6	80	4
310	16.5	230	40	6.0	270	57	1.6	100	3
330	15.6	180	42	6.5	230	56	2.1	80	2
350	14.7	140	46	6.9	180	54			

[a] The symbols have the same meaning as in Table I; [2,4-PD] = 2.28 M, [boron] = 0.05 M.

solution change with addition of the diol. These results do not allow us to specify which effect is the likely cause of horizontal shifts in the titration data. Close agreement between calculated curves and data points in Figure 7 does, however, support our interpretation of δ_f by using eq 5 and 6 for diol/SB solutions.

Temperature Dependence. Line widths and chemical shifts of the complexed-boron signals vary with pH in the 2,4-PD/SB system but are essentially constant for 2,3-BD/SB solutions (see Figure 8). These facts suggest that 2,4-PD/SB complexed-boron signals are affected by

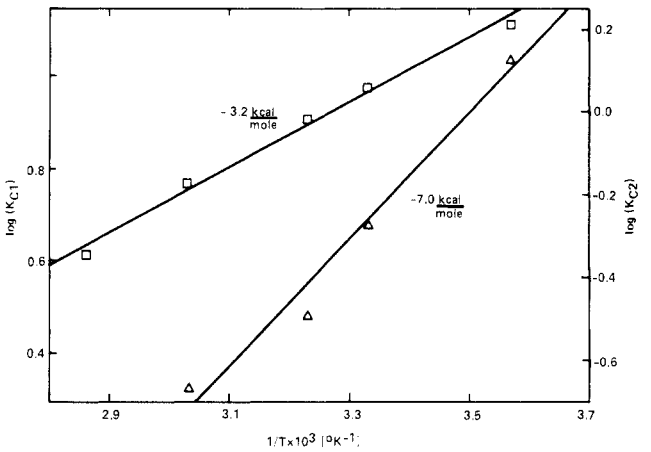

Figure 10. Logarithm of the complexation equilibrium constants (K_{C1} and K_{C2}) vs. inverse temperature for the 2,4-PD/SB system. Solid lines are the least-squares fits to the data for K_{C1} (squares) and K_{C2} (triangles).

chemical exchange and that this exchange is either absent or much slower in the 2,3-BD/SB case. NMR parameters at various temperatures for the 2,4-PD/SB solution with the highest diol concentration are listed in Table III. The peak assigned to 1:1 complexes (δ_1 in Table III) narrows with increasing temperature, as does the free-boron peak. Exchange between free and complexed forms of boron is evidently slow over the entire temperature range studied.

The temperature-dependent line widths of this system were interpreted with a model containing two fast-exchange processes: the free-boron species exchange rapidly according to eq 1 while boron in 1:1 complexes exchanges between trigonal and tetrahedral forms according to the equilibrium

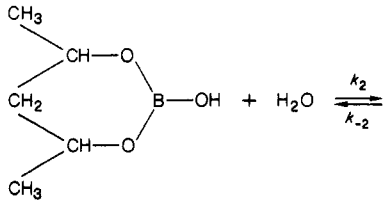

I′

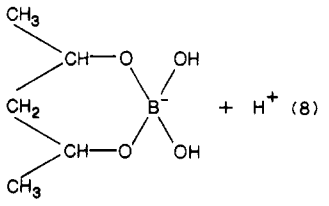

I

Exchange of boron between free and complexed forms is slow in comparison to these exchange processes. As before, K_a was taken as a constant over the temperature range of the experiment. Likewise, $K_a^{1:1}$, the equilibrium constant for eq 8, was assumed to be constant. The rate constants were calculated as described in the Appendix and are presented in the form of Arrhenius plots in Figure 9. The activation energies are $E_a^{free} = 8.6$ and $E_a^{1:1} = 2.9 \pm 0.2$ kcal/mol.

Linearity in the data points plotted in Figure 9 is an encouraging indication that the exchange model, despite the many assumptions necessary to complete the calculations, is basically correct. The activation energy for free-boron exchange is larger than for the pure SB case. This can be explained as a higher barrier to diffusion in the more viscous solution containing the organic liquid.

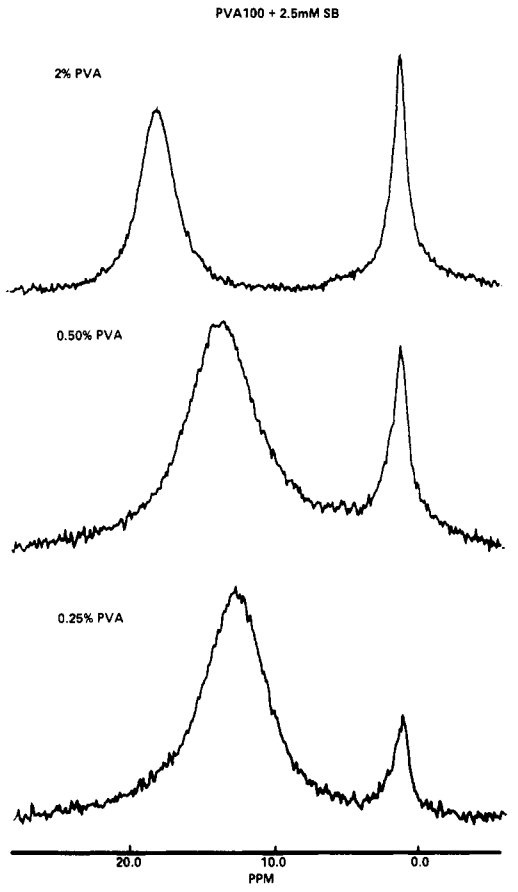

Figure 11. ^{11}B NMR spectra of 2.5 mM SB (0.01 M boron) in water with three different PVA100 concentrations, as indicated.

It is notable, however, that $E_a^{1:1}$ is much less than E_a^{free} even though both I and I′ are larger molecules than $B(OH)_3$ and $B(OH)_4^-$. This can only be explained if there is a chemically controlled component of the activation energy which decreases with complexation: boron is a more acidic when complexed ($pK_a^{1:1}$ estimated from the data is about 8.5). Since the magnitude of $E_a^{1:1}$ depends on the assumed values for intrinsic line widths of compounds I and I′, this conclusion must be considered as a tentative one. The narrow complexed-boron line shapes in the 2,3-BD system could be the result of strong steric forces slowing or preventing exchange between different forms of the complexes.

The equilibrium constants K_{C1} and K_{C2} were calculated for each temperature from the data in Table III. The enthalpy contribution to the free energy of complexation can be extracted from the standard equations:

$$K_{C1} = \exp(-\Delta G_1/RT) \quad (9a)$$

$$K_{C2} = \exp(-\Delta G_2/RT) \quad (9b)$$

where

$$\Delta G_1 = \Delta H_1 - T\Delta S_1 \quad (10a)$$

$$\Delta G_2 = \Delta H_2 - T\Delta S_2 \quad (10b)$$

In these equations, the usual symbols for the free energy, enthalpy, and entropy appear, and subscripts refer to the two complexation reactions (eq 2 and 3). Figure 10 is a plot of log K_{C1} and log K_{C2} against $1/T$. The enthalpies ΔH_1 and ΔH_2 obtained from the slopes of the linear fits are −3.2 and −7.0 kcal/mol, respectively.

PVA/SB Complexation. Chemical-Shift Assignments. NMR spectra of 2.5 mM SB solutions with varying amounts of PVA100 appear in Figure 11. NMR parameters and viscosities for a number of solutions are given

Table IV
^{11}B NMR Parameters[a] and Viscosities for PVA/SB Solutions

% PVA[b]	η[c]/cP	δ_f	W_f	A_f	δ_c	W_c	A_c(broad)	A_c(narrow)
				PVA96				
2.00	4000	16.0	270	58	1.0	100	19	23
1.00	10	16.0	410	69	0.9	80	14	17
0.50	20	13.6	550	76	1.0	120	13	11
0.25	10	12.0	470	90	0.8	100	5	5
				PVA88				
2.00	4000	18.1	330	62	1.6	140	12	26
1.00	30	15.3	530	68	1.0	100	17	15
0.50	30	13.1	630	83	1.0	120	5	12
0.25	10	12.2	510	91	1.3	100	4	5
				PVA100				
2.00	90	17.9	230	63	1.0	80	17	18
1.00	20	16.1	410	68	1.1	100	16	16
0.50	10	13.5	490	82	1.0	100	7	11
0.25	10	13.9	470	93	1.3	100	3	4
				PVA98				
2.00	20	17.4	310	56	0.9	80	26	18
1.00	20	16.0	470	69	1.1	100	15	16
0.50	10	13.6	530	83	1.1	100	6	11
0.25	20	11.6	450	88	1.1	80	6	6

[a] δ_f, W_f, and A_f are the chemical shift, width, and relative area of the free-boron peak, respectively. δ_c, W_c, and A_c(broad), A_c(narrow) likewise refer to the complexed-boron signal. Only the width of the narrow component is given (W_c). The broad-component line width is between 300 and 600 Hz in each case. [b] PVA96, PVA88, PVA100, and PVA98 refer to the different polymer grades (see Experimental Section for a definition of these terms). Total boron concentration in all solutions was 0.01 M. [c] Viscosity at 10 s^{-1} shear rate.

in Table IV. The usual free-boron peak appears along with another peak at about 1 ppm. Assignment of this "complexed-boron" peak is discussed below. The free-boron line widths are similar to those in SB and diol/SB spectra while viscosities vary considerably. Diffusion and exchange of the boric and monoborate species and hence the free-boron line width, should depend on solvent viscosity as well as pH, concentration, and temperature. The apparent lack of correlation between W_f and η in Table IV is consistent with the view that the high viscosities arise from large, cross-linked, polymer networks suspended in a low-viscosity solvent. Titration experiments with PVA/SB solutions reveal a trend in pK_a with polyol concentration similar to the diol/SB case. For example, the effective value of pK_a for a 2% PVA100/2.5 mM SB solution was found to be 9.7 compared to 9.0 for SB alone. This effect on pK_a can probably explain the pH data of Nickerson,[13] which lead him to consider hydrogen bonding to be more important than complexation in this system.

Commercial polymerizations of vinyl acetate (the starting material in PVA synthesis) usually produce a small number of head-to-head monomer pairs which ultimately lead to a few percent of diads with 1,2-type hydroxyl substitution in the hydrolyzed PVA product.[21] From the 2,3-BD/SB data, one might expect these diads to complex monoborate in addition to 1,3-type diads. However, NMR signals at shifts matching complexed-boron chemical shifts of the 2,3-BD/SB system were not observed. Thus, complexation at 1,2-type sites is ignored in what follows.

The complexed-boron signal is actually composed of two components: a narrow peak and a much broader "foot" at about the same position. This is seen most clearly in spectra acquired during an inversion–recovery spin–lattice relaxation experiment and plotted in Figure 12. In this experiment, signals are first inverted and then allowed to relax back to their positive-intensity equilibrium condition. It can be seen from the spectra for intermediate values of the recovery time that the two complexed-boron signal components relax at different rates. From a nonlinear, least-squares analysis of these spectra, spin–lattice relaxation rates of 600 ± 200 s^{-1} and 80 ± 20 s^{-1} were calculated for broad and narrow complexed-boron components, respectively. Relaxation of the free-boron signal is accurately described by a single exponential function with a rate of 220 ± 20 s^{-1}.

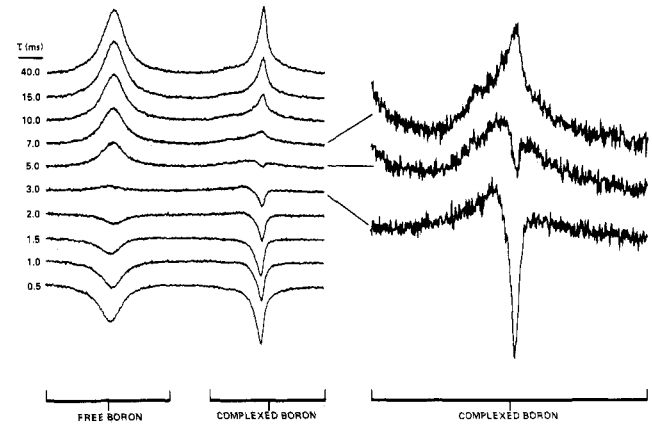

Figure 12. Inversion–recovery spectra from a solution of 2% PVA88/2.5 mM SB. The relaxation delay, τ, for each spectrum is indicated at the left. The complexed-boron regions of spectra at three intermediate values of τ are expanded on the right to emphasize the two components (broad and narrow) which relax at different rates.

The complexed-boron line shape and relaxation features contain information about molecular motions in the PVA/SB system. It should be recalled that quadrupolar nuclei such as ^{11}B ($I = {}^3/_2$) will exhibit multiexponential spin–lattice and spin–spin relaxation except under conditions of extreme narrowing.[27,28] Thus, the PVA/SB complexed-boron signal could possibly arise from a single chemical species undergoing sufficiently slow motions so that relaxation is not a single exponential decay. However, it is clear from Figure 12 that there are possibly two complexed-boron species and that exchange of ^{11}B between these species is slow compared to their relaxation rates. Both the broad and narrow components of the complexed-boron signal are close to Lorentzian line shapes which indicates that extreme narrowing could apply for individual species. Spin–spin relaxation rates estimated from the line widths are greater than the rates measured for spin–lattice relaxation (above). Although this fact argues against ex-

treme narrowing of the complexed-boron signals, it does not rule this out completely as these signals are susceptible to chemical-exchange broadening as in the 2,4-PD/SB system.

The broad and narrow components of the complexed-boron signal might arise from complexes of different stoichiometry (i.e., 1:1 and 2:1 complexes). One would then expect the ratio of their areas to vary with PVA concentration and temperature. These areas were estimated by fitting each spectrum with two Lorentzian line shapes at the position of the complexed-boron peak. The results are given as A_C(broad) and A_C(narrow) in Tables IV and V. In almost every case, relative amounts of the two components are nearly equal. Deviations from this general description could easily be explained as imprecision in the peak-area fits and do not necessarily indicate concentration variations. Thus, both components most likely arise from complexes with equivalent stoichiometry. The chemical shift of both components does not vary much with concentration, pH, or temperature and its value (1 ppm) indicates tetrahedral boron. This situation is most analogous to the 2:1 peak in the 2,4-PD/SB system. Thus, both components are assigned to 2:1-type complexes. Additional evidence for this assignment is given below. In the discussion which follows, I refer to these complexes as cross-links and assume that they either connect different segments of the same polymer chain (intramolecular cross-links) or different chains (intermolecular crosslinks). If the motions responsible for relaxation of the nuclei involve movement of large, cross-linked networks, then one would expect some correlation between the complexed-boron line shapes and bulk viscosity. Since no such correlation clearly exists, it can be concluded that the motions important in spin relaxation probably involve local molecular mobility such as segmental motions of the polymer chain or the mobility of molecules which are not part of the viscosity-determining network.

If the assignments above are correct, then the spectra show no evidence for 1:1 complexes in PVA/SB solutions. A signal from boron in these complexes might be simply too broad to detect or, alternatively, the equilibria could strongly favor 2:1 complexes. One can understand how the latter situation might come about by considering complexation in a stepwise manner. Each 1:1 complex that forms has a high probability of enountering a second meso diad within the highly concentrated "random-coil" volume of the chain. If this is correct, then most 1:1 complexes will react further to form intrachain cross-links. Interchain cross-links can form if different chains are in close enough proximity that this reaction competes with intrachain cross-linking. The question naturally arises as to how cross-links are distributed between these two varieties for different polymer molecular weights. This question is addressed next.

Viscosity Trends. Viscosities are generally low and mildly dependent on polymer concentration except for the higher MW grade PVAs. For these polymers, viscosities jump more than 2 orders of magnitude as concentration changes from 1 to 2%. In fact, 2% PVA88 and 2% PVA96 solutions with 2.5 mM SB have the appearance of loose gels and exhibit elastic properties. Interchain cross-linking must build large polymer networks (and, hence, high viscosity) in these solutions. The fraction of 2:1 complexes which connect different chains evidently depends on both polymer MW and concentration. If the peak areas of Table IV account for all the boron present, then the percentage of boron which is in cross-links (A_C(broad) + A_C(narrow) in Table IV) depends on PVA concentration

Table V
Temperature Dependence of NMR Parameters for 2% PVA100/2.5 mM SB[a]

T/K	δ_f	W_f	A_f	δ_c	W_c	A_c(broad)[b]	A_c(narrow)[b]
278	18.9	220	61	0.9	40	28	11
283	18.7	220	59	1.0	60	20	18
300	17.8	230	63	1.0	80	19	18
310	17.4	220	65	0.9	80	19	16
330	16.3	200	73	1.0	80	16	11
350	15.8	140	86	0.9	100	6	14

[a] Symbols for shifts, line widths, and peak areas are the same as in Table IV. [b] A_c(broad) and A_c(narrow) were obtained by fitting the complexed-boron line shape with two Lorentzian lines such that the sum of the individual areas equals the relative area of the complexed-boron signal obtained by standard integration techniques. The width of the broad-component Lorentzian is between 300 and 600 Hz in each case.

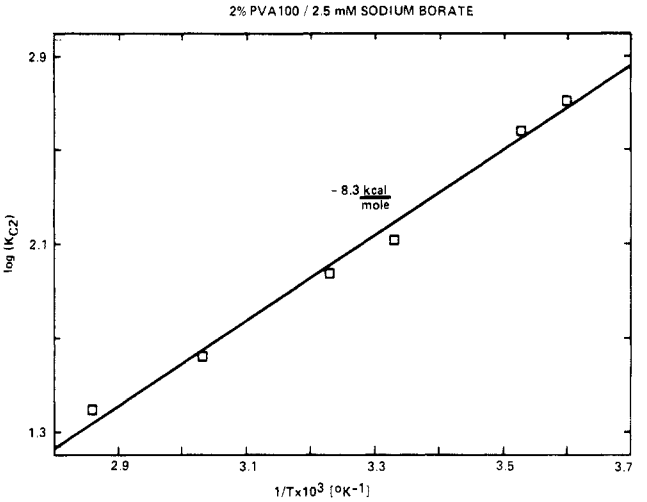

Figure 13. Plot of log K_{C2} vs. inverse temperature obtained from Table V for 2% PVA100/2.5 mM SB. The enthalpy from the slope of the linear fit is −8.3 kcal/mol.

but not on molecular weight. This seems reasonable since the complexation equilibria should depend on monomer concentration (moles of vinyl alcohol per liter of solution) and not on the degree of polymerization. Thus, formation of interchain cross-links is at the expense of intrachain cross-links while the overall equilibrium between free and complexed boron is maintained. Of course, small variations (on the order of 10%) in the complexed-boron concentration may be undetectable, given the precision of the peak-area determinations.

Temperature Dependence. As in the 2,4-PD/SB case, PVA complexation is exothermic: The fraction of complexed boron decreases with increasing temperature as seen for PVA100 in Table V. Equilibrium constant K_{C2} was calculated from these data by using the sum A_C(broad) + A_C(narrow) to define total cross-link concentration. The logarithm of K_{C2} calculated in this manner is plotted against inverse temperature in Figure 13. The linear fit in this figure has a slope corresponding to an enthalpy of −8.3 kcal/mol. The calculations were repeated with cross-link concentration determined from either A_C(broad) or A_C(narrow) alone. Scatter in log K_{C2}against $1/T$ plots for these two cases is greater than that in Figure 13 but linear fits were nevertheless obtained corresponding to enthalpies of −9.9 kcal/mol (broad component) and −7.1 kcal/mol (narrow component). Because of uncertainty in peak-area determinations, differences among these values do not necessarily indicate specific chemical effects. For each treatment of the data, however, the magnitude found for the complexation enthalpy is most similar to ΔH_2 of

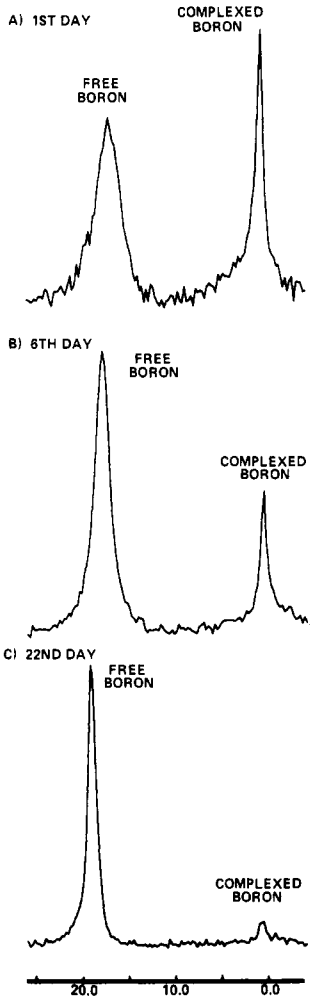

Figure 14. ^{11}B spectra of 2% PVA88/2.5 mM SB at various times following initial mixing of reagents. The fraction of boron complexed decreases with time concurrently with a decrease in viscosity.

the 2,4-PD/SB system. This supports the assignment of complexed-boron signals from PVA/SB solutions to cross-links.

Schultz and Myers[12] reported a value of −5 kcal/mol for ΔH_2 calculated from dynamic mechanical data on borate-cross-linked PVA gels at various temperatures. They used sodium metaborate as the cross-linking agent and assumed that monoborate concentration was independent of temperature in their calculations. This assumption would clearly not be valid for the PVA/SB system. If monoborate concentration actually varied with temperature in the experiments of Schultz and Myers, including this effect in their calculations would probably cause the magnitude of ΔH_2 to increase. This may account for the discrepancy in enthalpies determined by the NMR method and dynamic mechanical measurements.

Long-Term Stability. The discussion so far has assumed that the polymer solutions are equilibrium systems. However, when made with partially hydrolyzed PVA, solution properties do change over time periods on the order of days. Figure 14 shows the time variations of ^{11}B spectra for 2% PVA88/2.5 mM SB. Viscosity of this solution dropped exponentially from an initial value on the order of 4000 cP to about 10 cP in a 21-day period. The final viscosity is close to that of a 2% PVA 88 solution with no SB. One might suspect slow relaxation of a polymer network with concomitant decrease in cross-link concentration as the explanation of this behavior. This is inconsistent with the observed increase in δ_f. Instead, the loss of complexation is attributed to a decrease in pH with time. Similar pH decreases with time were noted even after extensive efforts to exclude carbon dioxide from the solutions. When fully hydrolyzed PVA is used, pH remains fairly constant with time.[14] The most likely cause for the pH drop with partially hydrolyzed PVA solutions is slow hydrolysis of the polymer molecules. This is known to occur under alkaline conditions.[29]

Concluding Remarks

NMR clearly gives useful information on the chemistry of polyol/SB complexation. I believe these results constitute the first determination of equilibrium constants and enthalpies for the PVA/SB system by a spectroscopic method. The NMR method is sensitive, rapid, and, in a sense, more direct than either mechanical or pH methods. Differences among results from these methods were explored, and I conclude that NMR provides several advantages, most notably the simultaneous determination of all relevant concentrations without the need for a separate pH determination.

At the concentrations studied, exchange rates were sufficiently slow to allow determination of activation energies related to exchange of boron (free and 1:1 complexed) between trigonal and tetrahedral forms. It should be possible to resolve the issue of whether diffusional or chemical barriers dominate activation energies by carefully studying how exchange rates vary with viscosity and temperature. Exchange rates between free and complexed boron were very slow (relative to chemical shift differences) in all solutions and at all temperatures investigated. Schultz and Myers calculated a value of 6 kcal/mol for the activation energy required to break PVA–borate complexes.[12] This is in the range of activation energies measured for fast-exchange processes in our study. Considering the changes in chemical shifts which might accompany breakup of a complex, a barrier of only 6 kcal/mol should lead to a fast-exchange condition. This is inconsistent with all the observations. Thus, the activation energy reported by Schultz and Myers seems somewhat low in light of these new results, although it cannot be rejected entirely.

Reaction enthalpies on the order of −3 and −7 kcal/mol for 1:1 and 2:1 complexation were found for 2,4-PD. These figures compare reasonably well since one expects about equal enthalpy changes for each step in the formation of 2:1 complexes ($B^- \rightarrow AB^- \rightarrow A_2B^-$). The PVA system has a slightly larger enthalpy of formation for cross-links. Structure II was confirmed for these cross-links by comparing diol/SB and PVA/SB spectra. Finally, evidence that there are possibly two types of cross-links was discovered. Relaxation data indicate that if there are two types of cross-links, they experience different local molecular motions. Although one might be tempted to call these two types intrachain and interchain cross-links, such an assignment cannot be made unequivocally.

There are a number of molecular theories which attempt to relate cross-link concentration and lifetimes to viscosity of polymer solutions. Quantitative molecular information, when combined with rheology, offers the potential for testing predictions and perhaps choosing between competing theories. Discussions of NMR data on PVA/SB solutions in terms of molecular theories of viscosity are given elsewhere.[14] In this sense, the PVA/SB system is a valuable model system for "associating" polymers in general, of which there are now a number of well-characterized examples.

Some of these polymer systems (including PVA/SB) exhibit pronounced shear-thickening characteristics.[14,30]

Witten and Cohen[31] developed a theory to explain shear-thickening phenomena of associating polymer solutions. The important chemical and physical considerations are (i) the strength of the associations, (ii) association lifetime, and (iii) equilibria between intrachain and interchain associations. Their theory addresses a case where association strengths are large compared to mechanical and thermal energies, the total number of associations is constant, and association lifetimes are longer than hydrodynamic relaxation times. Shear-thickening behavior is seen to be a result of a shift in the equilibrium between intrachain and interchain associations as polymer molecules become elongated by shear. The present study indicates that the PVA/SB system fits this picture of polymer association, at least a far as association strengths and lifetimes are concerned. NMR can potentially measure equilibrium constants as a function of shear if experiments can be performed on flowing samples. This could allow one to determine whether the flow behavior of this system results from a shift in the overall equilibrium between free and complexed boron or a shift in only the relative amounts of intrachain and interchain cross-links.

Acknowledgment. I am indebted to J. M. Maerker, T. A. Witten, P.-G. de Gennes, A. S. Lodge, and R. A. Smith for many helpful discussions and suggestions. I also acknowledge the technical assistance of B. E. Boeger, who made the rheological measurements, and M. Savage and P. Z. McCammon, for assistance with the NMR experiments.

Appendix

Two-Site Exchange Model. General Case. The treatment of chemical exchange effects on ^{11}B NMR line shapes follows the theory of Hahn and Maxwell[32] and McConnel,[33] which was originally developed for protons but should also be useful for spin-$^3/_2$ nuclei (i.e., ^{11}B) in isotropic solution. This theory has been reviewed elsewhere,[34] and I only cite the relevant results below. This treatment is applicable to the case where ^{11}B nuclei are exchanging between two dissimilar magnetic sites according to eq A.1 where k_f and k_r are the rate constants.

$$B_1 \underset{k_r}{\overset{k_f}{\rightleftharpoons}} B_2 \tag{A.1}$$

The line-shape function in this situation is a complicated expression involving chemical shifts and line widths of the pure species and the rate at which they exchange. Above the so-called coalescence temperature, where the line shape changes from two separate peaks to a single peak, the rate constants are given approximately by the expressions

$$k_f = \frac{p_1 p_2{}^2 4\pi(\nu_1 - \nu_2)^2}{(W - W^*)} \tag{A.2}$$

$$k_r = \frac{p_2 p_1{}^2 4\pi(\nu_1 - \nu_2)^2}{(W - W^*)} \tag{A.3}$$

$$W^* = p_1 W_1 + p_2 W_2 \tag{A.4}$$

In these expressions, p_1 and p_2 are the fractions of boron of each type, ν_1 and ν_2 are their intrinsic chemical shifts (in units of hertz), W_1 and W_2 are their intrinsic line widths, and W is the observed line width. All of the data were taken at temperatures well above the coalescence temperature.

Free-Boron Exchange. The site fractions for this case can be calculated by solving eq 4 and 6 for X_B and X_{B^-} where these mole fractions are relative to the total free-boron concentration. Equations A.2 and A.3 are appropriately modified to reflect the fact that the exchange rate depends on pH:

$$k_1 = k_{-1}K_a = \frac{X^2}{(1 + X)^3} \frac{4\pi(\nu_B - \nu_{B^-})^2}{(W - W^*)} \tag{A.5}$$

Intrinsic shifts and line widths were determined from spectra taken at extreme pH positions on the titration curve (Figure 2). Thus, $(\nu_B - \nu_{B^-}) = 1704$, $W_B = 70$, and $W_{B^-} = 40$ Hz.

Complexed-Boron Exchange. Intrinsic shifts and line widths are not available for pure 1:1 complexes with structures I and I′. Instead, it is assumed that these are the same as for the free-boron species. The approach to calculating species fractions is the same as in the free-boron case with k_2, k_{-2}, and $K_a{}^{1:1}$ substituted for k_1, k_{-1}, and K_a in eq A.5. The assumed values for intrinsic shifts and widths may not be entirely justified, but as pointed out in the text, a reasonably Arrhenius plot results when this model is used to interpret the data.

Equilibrium Constant Calculations. Diol/SB Case. The equilibrium constants for complexation of monoborate anions with organic diol are defined as

$$K_{C1} = \frac{[AB^-]}{[A][B^-]} \tag{A.6}$$

$$K_{C2} = \frac{[A_2B^-]}{[A]^2[B^-]} \tag{A.7}$$

The mass balance equation applicable to this case is

$$[A] = [A]_0 - [AB^-] - 2[A_2B^-] \tag{A.8}$$

where $[A]_0$ is the total meso-isomer concentration. This concentration is assumed to be one-half of the total diol concentration for isomer mixtures. Monoborate concentration is calculated from δ_f and p_f, the fraction of free boron, as

$$[B^-] = \frac{X}{(1 + X)} p_f [B]_0 \tag{A.9}$$

where $[B]_0$ is the total boron concentration. Concentrations of 1:1 and 2:1 complexes are calculated from the peak areas and $[B]_0$.

PVA/SB Case. Equations A.6 and A.7 again define the equilibrium constants with [A] now referring to the uncomplexed meso-diad concentration. Since the polymers are atactic, the total concentration of meso diads is taken to be just one-half the monomer concentration (each monomer is actually part of two diads). This is strictly true only for completely hydrolyzed PVA. The meso-diad concentration in the variable-temperature experiment with 2% PVA100/2.5 mM SB far exceeds complexed-boron concentration so that the mass balance equation becomes

$$[A] \sim [A]_0 = \tfrac{1}{2}[\text{monomer}] \tag{A.10}$$

The monoborate concentration is calculated from eq A.9 as in the diol/SB case.

Registry No. 2,4-PD, 625-69-4; 1,5-PD, 111-29-5; 2,3-BD, 513-85-9; SB, 1303-96-4; (SB)(VA) (copolymer), 109720-01-6.

References and Notes

(1) Farmer, J. B. *Adv. Inorg. Chem. Radiochem.* Academic: **1982**, *25*, 187.
(2) Ingri, N. *Acta Chem. Scand.* **1962**, *16*, 439.
(3) Roy, G. L.; Lafferjer, A. L.; Edwards, J. O. *J. Inorg. Nucl. Chem.* **1957**, *4*, 106.
(4) Kustin, K.; Pizer, R. *J. Am. Chem. Soc.* **1969**, *91*, 317.
(5) Oertal, R. P. *Inorg. Chem.* **1972**, *11*, 544.
(6) Pizer, R.; Babcock, L. *Inorg. Chem.* **1977**, *16*, 1677.

(7) Paal, T.; Kenez, M. D. *Magy. Kem. Foly.* **1980**, *86*, 218.
(8) Henderson, W. G.; How, M. J.; Kennedy, G. R.: Mooney, E. F. *Carbohydr. Res.* **1973**, *28*, 1.
(9) Yoshino, K.; Kotaka, M.; Okamoto, M.; Kakihana, H. *Bull. Chem. Soc. Jpn.* **1979**, *52*, 3005.
(10) Pasdeloup, M.; Brisson, C. *Org. Magn. Reson.* **1981**, *16*, 164.
(11) Savins, J. G. *Rheol. Acta* **1968**, *7*, 87.
(12) Schultz, R. K.; Myers, R. R. *Macromolecules* **1969**, *2*, 281.
(13) Nickerson, R. F. *J. Appl. Polym. Sci.* **1971**, *15*, 111.
(14) Maerker, J. M.; Sinton, S. W. *J. Rheol.* **1986**, *30*, 77.
(15) Noth, H.; Wrackmeyer, B. *NMR: Basic Princ. Prog.* **1978**, *14*.
(16) Onak, T. P.; Landesman, H.; Williams, R. E.; Shapiro, I. *J. Phys. Chem.* **1959**, *63*, 1533.
(17) Wolf, R. M.; Suter, U. W. *Macromolecules* **1984**, *17*, 669.
(18) Inoue, Y.; Chujo, T.; Nishioka, A. *J. Polym. Sci.* **1973**, *11*, 393.
(19) Wu, T. K.; Ovenall, D. W. *Macromolecules* **1973**, *6*, 582.
(20) Wu, T. K.; Sheer, M. L. *Macromolecules* **1977**, *10*, 529.
(21) Ovenall, D. W. *Macromolecules* **1984**, *17*, 1458.
(22) Momii, R. K.; Nachtrieb, N. H. *Inorg. Chem.* **1967**, *6*, 1189.
(23) Smith, H. D., Jr.; Wiersema, R. J. *Inorg. Chem.* **1972**, *11*, 1152.
(24) Covington, A. K.; Newman, K. E. *J. Inorg. Nucl. Chem.* **1973**, *35*, 3257.
(25) Janda, R.; Heller, G. *Z. Naturforsh., B* **1979**, *34B*, 1078.
(26) Salentine, C. G. *Inorg. Chem.* **1983**, *22*, 3920.
(27) Abragam, A. *The Principles of Nuclear Magnetism*; Oxford: London, 1961; Chapter 8.
(28) Wennerstrom, H.; Lindblom, G.; Lindman, B. *Chem. Scr.* **1974**, *6*, 97.
(29) Modi, T. In *Handbook of Water-Soluble Gums and Resins*; Davidson, R. L., Ed.; McGraw-Hill: New York, 1980; Chapter 20.
(30) Agarwal, P. K.; Makowski, H. S.; Lundberg, R. D. *Macromolecules* **1980**, *13*, 1679.
(31) Witten, T. A.; Cohen, M. H. *Macromolecules* **1985**, *18*, 1915.
(32) Hahn, E. L.; Maxwell, D. E. *Phys. Rev.* **1952**, *88*, 1070.
(33) McConnell, H. M. *J. Chem. Phys.* **1958**, *28*, 430.
(34) Sutherland, I. O. In *Annual Reports on NMR Spectroscopy*; Mooney, E. F., Ed.; Academic: New York, 1971.

High-Resolution ^{15}N NMR Study of Solid Homopolypeptides by the Cross-Polarization–Magic Angle Spinning Method: Conformation-Dependent ^{15}N Chemical Shifts Characteristic of the α-Helix and β-Sheet Forms

Akira Shoji* and Takuo Ozaki

Department of Industrial Chemistry, College of Technology, Gunma University, Tenjin-cho, Kiryu, Gunma 376, Japan

Teruaki Fujito and Kenzo Deguchi

NM Group, Analytical Instruments Technical and Engineering Division, JEOL Ltd., Nakagami, Akishima, Tokyo 196, Japan

Isao Ando

Department of Polymer Chemistry, Tokyo Institute of Technology, Ookayama, Meguro-ku, Tokyo 152, Japan. *Received February 3, 1987*

ABSTRACT: Natural abundance 27.4-MHz ^{15}N NMR spectra of various homopolypeptides having right-handed α-helix (α_R-helix) and β-sheet conformations in the solid state were measured by using the cross-polarization–magic angle spinning (CP-MAS) technique. It was found that the ^{15}N chemical shifts in the peptide backbone of these polypeptides exhibit a significant conformation-dependent change. The α_R-helix conformation absorbs upfield of the β-sheet (α_R-helix form δ 97.0–99.2; β-sheet form δ 99.5–107.0). Furthermore, the ^{15}N chemical shift was found to be displaced by as much as 1.2–10.0 ppm between the α_R-helix and β-sheet forms, depending on the nature of the amino acid residue.

Introduction

^{15}N NMR spectroscopy offers many possibilities for study on the structure and dynamics of synthetic polypeptides and natural proteins.[1-6] Recently, a high-resolution ^{15}N NMR technique in the solid state has been increasingly applied to the investigation of polypeptides, proteins, and biopolymers.[7-14] However, with the exception of the group of Kricheldorf,[10] little attempt has been made to relate the ^{15}N chemical shift to conformational features such as the secondary structure determined by the peptide bonds of the backbone. The secondary structure plays a particularly important role in such a system and enables us to test if the ^{15}N chemical shifts can be examined as a possible source of information about the microstructures of solid polypeptides and proteins with these spectra. This is because, in polypeptides and proteins, most of the nitrogen sites are in the amide linkage of the backbone and also because the structure and dynamics of the backbone strongly reflect the conformation and the flexibility of these macromolecules. Kricheldorf and co-workers have reported extensively that ^{15}N NMR in solution can be used to determine sequence distributions of polypeptides.[15-19] It should be mentioned that comparisons between the solid and solution ^{15}N NMR spectra give us some information concerning the conformational difference between the solid and solution states.

In previous investigations,[18-35] it has been demonstrated that the ^{13}C NMR chemical shifts of a number of polypeptides and proteins in the solid state as determined by the CP-MAS method are significantly displaced depending on their particular conformations, such as α-helix, β-sheet, 3_1-helix, collagen-like triple helix, ω-helix, and so on. In particular, the ^{13}C chemical shifts of an individual amino acid residue in a peptide or protein are mainly influenced by the local conformation, as defined by the torsional angles (ϕ and ψ) of the skeletal bonds, and not strongly influenced by the specific amino acid sequence.[18,19,24-26,30] This view was supported by our theoretical calculations of the contour map of the ^{13}C chemical shift utilizing the finite perturbation (FPT)-INDO theory[23,27] and the sum-over-states tight-binding MO theory.[28,29] These approaches permit one to use the conformation-dependent ^{13}C chem-

0024-9297/87/2220-2441$01.50/0